

Published in final edited form as:

Nat Neurosci. 2009 October ; 12(10): 1333–1342. doi:10.1038/nn.2401.

Transformation of nonfunctional spinal circuits into functional states after the loss of brain input

Grégoire Courtine^{1,2}, Yury Gerasimenko^{3,4}, Rubia van den Brand^{1,2}, Aileen Yew⁵, Pavel Musienko^{1,2,4}, Hui Zhong³, Bingbing Song⁶, Yan Ao⁶, Ronaldo M Ichiyama³, Igor Lavrov³, Roland R Roy^{3,6}, Michael V Sofroniew^{5,6}, and V Reggie Edgerton^{3,5,6}

¹Neurology Department, University of Zurich, Zurich, Switzerland ²Rehabilitation Institute and Technology Center Zurich, Zurich, Switzerland ³Department of Physiological Science, University of California Los Angeles, Los Angeles, California, USA ⁴Motor Physiology Laboratory, Pavlov Institute of Physiology, St. Petersburg, Russia ⁵Department of Neurobiology, University of California Los Angeles, Los Angeles, California, USA ⁶Brain Research Institute, University of California Los Angeles, Los Angeles, California, USA

Abstract

After complete spinal cord transections that removed all supraspinal inputs in adult rats, combinations of serotonergic agonists and epidural electrical stimulation were able to acutely transform spinal networks from nonfunctional to highly functional and adaptive states as early as 1 week after injury. Using kinematics, physiological and anatomical analyses, we found that these interventions could recruit specific populations of spinal circuits, refine their control via sensory input and functionally remodel these locomotor pathways when combined with training. The emergence of these new functional states enabled full weight-bearing treadmill locomotion in paralyzed rats that was almost indistinguishable from voluntary stepping. We propose that, in the absence of supraspinal input, spinal locomotion can emerge from a combination of central pattern-generating capability and the ability of these spinal circuits to use sensory afferent input to control stepping. These findings provide a strategy by which individuals with spinal cord injuries could regain substantial levels of motor control.

Severe spinal cord injuries that remove all supraspinal input to lumbosacral spinal circuits lead to permanent paralysis of the legs in adult rodents^{1–3} and humans. Nevertheless, networks of neurons in the lumbosacral spinal cord retain an intrinsic capability to oscillate and generate coordinated rhythmic motor outputs. Circuits underlying such rhythmic and oscillatory outputs are commonly referred to as central pattern generators (CPGs) and are found in all invertebrate and vertebrate animals^{4,5}. Although the anatomical architecture of locomotor CPGs remains poorly understood, especially in mammals⁵, the functional phenomenon, central pattern generation, has been documented extensively. Indirect evidence suggests that CPGs are present in human spinal cord^{6,7}. These observations offer the possibility of directly accessing and activating spinal cord CPGs to facilitate locomotor recovery after a severe spinal cord injury (SCI).

Correspondence should be addressed to G.C. (gregoire.courtine@bli.uzh.ch).

Note: Supplementary information is available on the Nature Neuroscience website.

Author Contributions: G.C., Y.P.G., I.L., M.V.S. and V.R.E. designed the study. G.C., R.R.R., H.Z. and P.M. performed the surgeries. G.C., Y.P.G., R.v.d.B., P.M. and A.Y. carried out the experiments. G.C., A.Y., B.S., Y.A., R.I. and M.V.S. conducted the anatomical assessments. G.C. analyzed the data. G.C., R.R.R., M.V.S. and V.R.E. wrote the manuscript. G.C. supervised the study.

Several experimental strategies have been tested to activate locomotor circuits in mammals after a complete spinal cord transection, including pharmacological treatments^{8–10}, epidural^{2,11,12} or intraspinal^{13,14} electrical stimulation, and motor training^{1,2,8,15,16}. Serotonin or agonists of 5-HT_{2A} and 5-HT_{1A/7} receptors can activate the quiescent locomotor circuitry in neonatal rodent fictive locomotion preparations^{17,18} and can facilitate treadmill stepping with limited weight bearing in adult rats⁹ and mice¹⁰ with SCI. Epidural electrical stimulation (EES) applied dorsally at the lumbar (L2)^{2,11} or sacral (S1)^{12,19} spinal segments induces rhythmic hindlimb movements^{2,12}. Locomotor training, notably in conjunction with pharmacological^{8,9} or electrical stimulation² interventions, can promote use-dependent plastic changes in sensorimotor circuits below the injury^{16,20,21} that lead to specific improvements of stepping patterns. These interventions, however, have shown limited potential for promoting weight-bearing capacities and there have been few attempts to correlate the specific functional states induced pharmacologically^{9,10}, electrically^{11–13,19,22} or by locomotor training^{2,20} with distinct characteristics of stepping motor patterns. When studied in sufficient statistical detail, analyses of kinematics and electromyographic (EMG) features revealed that such induced spinal locomotion differed from voluntary stepping in many important aspects^{2,9,13}. In addition, it remains unknown whether lumbosacral neuronal networks in the absence of brain input could sustain full weight-bearing locomotion that resembles nondisabled stepping. Considering the diffusely distributed⁵ and heterogeneous⁴ character of the spinal locomotor system, it is likely that multiple complementary approaches, both acute and chronic, would be required to attain the full possible expression of effective stepping in the absence of supraspinal input.

We tested the hypothesis that combinations of specific pharmacological and electrical stimulation interventions, together with locomotor training, may interact synergistically to activate and functionally remodel spinal locomotor circuits, possibly enabling a coordinated and context-dependent function of the paralyzed hindlimbs of adult rats after a complete spinal cord transection. We tested combinations of 5-HT_{2A} and 5-HT_{1A/7} serotonin agonists and EES at two different positions distal to the lesion, each of which individually exerted some facilitating effects on hindlimb function. Using detailed kinematics, EMG and anatomical analyses, we found that such combinatorial interventions induced unique functional states that correlated with distinct patterns of locomotion in paralyzed rats. We demonstrate for the first time, to the best of our knowledge, the ability of rats with SCI to generate full weight-bearing bipedal treadmill locomotion that is almost indistinguishable from voluntary stepping recorded in the same rats prior to injury. We also found that sensory input determines the formation of adaptive motor patterns in the absence of supraspinal influences.

Results

Experiments were conducted on adult rats that received a complete mid-thoracic (~T7) spinal cord transection, permanently removing all supraspinal input below the level of the lesion. At 7–8 d after injury, all of the rats showed flaccid paralysis of the hindlimbs; no bursts of EMG were observed in extensor or flexor muscles (Fig. 1) when a rat was positioned in a bipedal posture on a moving treadmill belt (9 cm s^{-1}) while secured in a jacket that was attached to a robotic arm used to control and measure the amount of hindlimb body weight support (BWS; Supplementary Fig. 1)².

Accessing spinal locomotor circuits

We first examined the ability of combined pharmacological and electrical stimulations to transform spinal circuits from a dormant to a functional state. These experiments were conducted sequentially (Fig. 1a–i) on the same rats to identify the specificity of and synergy between each intervention on the modulation of stepping patterns (Supplementary Fig. 2). To

facilitate stepping with electrical stimulation, we applied EES over the dorsal surface of L2 and S1 (Supplementary Fig. 1). We previously found that stimulation at either site can facilitate treadmill locomotion in paralyzed rats with SCI after 5–7 weeks of recovery post-injury^{11,19}. Applied 7–8 d post-injury, EES (40–50 Hz, 0.2 ms, 1–4 V) at L2 and/or S1 modestly increased EMG bursting patterns or tonic activity in the hindlimb muscles ($P < 0.05$; Fig. 2), but failed to generate any step-like movements (Fig. 1c). To engage locomotor networks pharmacologically, we administered quipazine, a predominantly 5-HT_{2A} receptor agonist, and 8-OHDPAT, a 5-HT_{1A} and 5-HT₇ receptor agonist. Both serotonin agonists can facilitate treadmill locomotion in spinal rodents after some weeks of recovery from SCI^{9,10}, but when systemically administered at 7–8 d post-injury, quipazine (0.3 mg per kg of body weight, intraperitoneal) and/or 8-OHDPAT (0.1–0.3 mg per kg, subcutaneous) induced only brief periods of erratic hindlimb movements in response to treadmill motion (Fig. 1f), with limited weight bearing (Fig. 2c) and small EMG bursts in both extensor and flexor muscles (Fig. 2g,h). Thus, pharmacological or EES interventions alone, administered 1 week after a complete interruption of supraspinal input, could not induce functional states that would enable stepping. In contrast, several combinations of serotonin agonists and EES were strongly synergistic, resulting in hindlimb locomotion whose features clearly varied with the procedures used (Fig. 1d–i).

We extensively quantified the kinematics and EMG characteristics of stepping movements caused by specific treatment combinations ($n = 135$; Supplementary Table 1). However, because a large number of these parameters changed substantially across combinations, we resorted to principal component analysis (PCA) to identify the specific contributions of individual interventions to the observed variations in hindlimb stepping. PCA transforms the raw dataset to a new coordinate system such that the explained variance is maximized on each axis. In the PCA-based statistical representation, the differences between gait patterns are related to the distance between the data points. The distinct spatial locations ($P < 0.05$; Fig. 1k–m) occupied by each combination (Fig. 1j) indicated that each intervention promoted a specific pattern of hindlimb locomotion. The distinct characteristics captured by each component can be extracted from the analysis of factor loadings, that is, correlations between each variable and each component. To visualize factor loadings, we developed a color-coded representation that clearly highlighted the variables that cluster on each component (Fig. 1n). For example, principal component 3 (Fig. 1j) differentiated the effects of quipazine from the effects of the other interventions ($P < 0.05$; Fig. 1j). Variables associated with joint extension (variables 56, 57 and 76) and EMG activity of extensor muscles (soleus, $P < 0.01$; Fig. 2g) clustered on principal component 3 (Fig. 1n), indicating that quipazine primarily facilitated extension components. 8-OHDPAT was significantly more effective in facilitating rhythmic movements of the hindlimbs under EES at S1 plus L2 compared with quipazine (principal component 1, $P < 0.05$; Figs. 1k and 2b,e). However, stepping patterns were less variable ($P < 0.001$; Fig. 2e), showing markedly improved interlimb coordination ($P < 0.01$; Fig. 2b) and higher levels of weight bearing ($P < 0.01$; Fig. 2c) when combining quipazine, 8-OHDPAT and EES at either site. In turn, principal component 2 differentiated gait patterns under EES at the L2 versus S1 levels ($P < 0.001$; Fig. 1i). Analysis of the variables that clustered on principal component 2 (Fig. 1m) showed that EES at L2 facilitated flexion and resulted in an enhanced swing phase ($P < 0.01$; Fig. 2f), whereas EES at S1 was more biased toward extension.

To further investigate the modulation of hindlimb movements by site-specific EES, we compared the changes in limb postures produced by EES at L2 compared with EES at S1. During standing (20% weight bearing), EES at L2 (Fig. 3) induced a rapid flexion (mean duration to peak flexion, 263 ± 96 ms) at all joints ($P < 0.001$; Fig. 3c,d) that was maintained tonically during the duration of the stimulation (3 s). In contrast, EES at S1 promoted a progressive whole-limb extension (mean duration to peak extension, $1,050 \pm 361$ ms; $P < 0.001$; Fig. 3a,d) that persisted as long as the stimulation was continued (3 s) and was comparatively

slower ($P < 0.001$) and less stable than the effects of EES at L2. Next, we tested the effects of increasing intensity at L2 versus S1 during locomotion enabled by quipazine, 8-OHDPAT and dual-site EES. Gradually increasing the intensity of EES at L2 progressively increased hip flexion ($P < 0.05$; Fig. 3d), step height ($P < 0.05$; Fig. 3c) and foot velocity ($P < 0.05$) during swing. Opposite effects ($P < 0.05$; Fig. 3c,d) were obtained when increasing EES at S1 (Fig. 3b). Together, these results demonstrate that upper lumbar stimulation engages the circuits controlling flexion, whereas upper sacral stimulation primarily recruits the circuits controlling extension.

When EES was simultaneously applied to L2 and S1 in the presence of quipazine and 8-OHDPAT (Fig. 1i), the variability of stepping motion was reduced compared with EES application at either site alone ($P < 0.01$; Fig. 2e). Weight-bearing ability increased twofold ($P < 0.01$; Fig. 2c) and EMG activity in extensor and flexor muscles reached levels similar to those observed during voluntary locomotion recorded in the same rats pre-injury (Fig. 2g,h). Although some defects persisted, for example, toe dragging at swing onset ($P < 0.05$; Figs. 1d and 2a) and only partial weight-bearing ability ($P < 0.001$; Fig. 2c), the resulting locomotor patterns resembled voluntary stepping (Fig. 1a,i). These results indicate that there is a strong, synergistic potential for combined pharmacological and electrical stimulations to functionally engage spinal locomotor circuits as early as 1 week after a complete spinal cord transection, promoting weight-bearing locomotion with plantar placement of the paws in the hindlimbs of paralyzed adult rats (Supplementary Video 1).

Learning in spinal locomotor circuits

Next, we sought to optimize the use of spinal circuits for recovery of locomotor function in the absence of supraspinal input. To attain this goal, we subjected rats with SCI to the above pharmacological and/or EES interventions in combination with well-established rehabilitative locomotor training procedures. We hypothesized that use-dependent mechanisms would functionally remodel the pharmaco-electrically activated spinal circuits and further improve stepping ability.

We exposed the rats to 20-min locomotor training sessions every other day for 8 weeks, starting 7-8 d post-injury. Stepping was enabled by the full combination of serotonergic agonists and dual-site EES. We compared the locomotor performance of these rats (Fig. 4) with their performance measured at 1 week post-injury, before any training (Fig. 1i), with that of nontrained rats that received no pharmacological or electrical stimulation (Fig. 4a) and with that of rats trained with either the serotonin agonists (Fig. 4b) or dual-site EES (Fig. 4c) alone (Supplementary Fig. 2).

PCA (Fig. 4f-j) identified clusters of variables on each component (Fig. 4f) that allowed us to differentiate the effects of the various conditions on stepping abilities. Principal component 1 identified improved performance in rats that were trained with the full combination of serotonergic agonists and dual-site EES compared with nontrained rats and rats trained with either the serotonergic agonists or EES alone ($P < 0.01$; Fig. 4h). Principal component 2 highlighted the deterioration of stepping ability in nontrained rats after 8 weeks compared with the gait patterns recorded at 1 week post-injury ($P < 0.001$; Fig. 4i). Principal component 3 revealed the importance of combining the serotonergic agonists and EES for promoting stepping improvement with locomotor training ($P < 0.01$; Fig. 4j). Deterioration of stepping capacities in chronic nontrained rats (Fig. 4a) was made evident by the substantial increase in movement variability ($P < 0.001$; Fig. 2e), the loss of interlimb coordination ($P < 0.001$; Fig. 2b) and the partial coactivation of normally reciprocally activated flexor and extensor hindlimb muscles (Fig. 4a and Supplementary Fig. 3). In contrast, rats trained with the full combination of treatments (Fig. 4d) recovered the ability to sustain full weight-bearing locomotion (Fig. 2c) with kinematic profiles of hindlimb joint angles ($P > 0.2$; Fig. 2d) and limb endpoint trajectories

(Fig. 4d) that were nearly indistinguishable from those observed during voluntary bipedal treadmill stepping in the same rats pre-injury (Fig. 1a). Although locomotor training with the full combination did not completely prevent the hindlimb muscle atrophy that accompanies a SCI, the amount of muscle weight loss was significantly less (mean for all muscles, 14%) in trained versus nontrained rats ($P < 0.01$; Supplementary Fig. 4). Deterioration of locomotor performance was reduced in rats trained with either the pharmacological or EES intervention compared with nontrained rats ($P < 0.01$; Fig. 4i). However, locomotor training enabled by the individual interventions failed to promote substantial improvement in stepping ability.

We next investigated use-dependent plastic changes in the spinal circuits that mediate the observed functional improvements. To assess physiological changes, we chronically measured the efficacy of monosynaptic inputs to extensor and flexor motoneurons in awake standing (20% weight bearing) rats²³. The rats showed a significant decrease in the amplitude of monosynaptic responses in extensor motoneuron pools 1 week post-injury ($P < 0.05$; Fig. 5a), whereas these values were unchanged in flexor motoneuron pools (Fig. 5b) compared to pre-lesion values. Before the onset of locomotor training, no significant differences could be detected between the two groups ($P > 0.4$; Fig. 5a,b). After 9 weeks of the absence of weight bearing in non-trained injured rats, we observed no significant changes in the amplitude of the responses in flexor motoneuron pools (Fig. 5b), whereas there was a moderate facilitation of the extensor motoneuron pools ($P < 0.05$; Fig. 5a). In contrast, after 8 weeks of locomotor training, all of the rats demonstrated a substantial increase in the efficacy of monosynaptic inputs to both extensor ($P < 0.01$; Fig. 5a) and flexor ($P < 0.01$; Fig. 5b) motoneuron pools. We further assessed the functional remodeling of lumbosacral locomotor networks anatomically by examining FOS expression patterns² induced by 45 min of continuous bipedal stepping under the full combination of treatments. Although FOS-positive nuclei were found mainly in laminae I–IV in the vicinity of the site of stimulation when EES was delivered with the rats in a prone, suspended non-weight-bearing position (Supplementary Fig. 5), FOS-positive nuclei were present in all of the laminae of the examined lumbar and sacral segments in response to locomotor activity (Fig. 5c,d). However, the number of FOS-positive cells per segment (L1 to S2) was two- to threefold higher in nontrained than in trained ($P < 0.01$) and noninjured ($P < 0.001$) rats (Fig. 5d and Supplementary Fig. 5). Moreover, the total number of FOS-positive cells was inversely correlated with the level of locomotor recovery ($P < 0.001$; Fig. 5e). These results confirm earlier observations² that motor learning can occur in adult rodent lumbosacral circuits after a complete spinal cord transection and extend these findings by showing that, in the absence of any supraspinal input, use-dependent learning mechanisms can promote the recovery of full weight-bearing treadmill locomotion that is kinematically very similar to pre-injury voluntary stepping in the same rats (Supplementary Video 2).

Control of spinal locomotor circuits

We next investigated how successful control of spinal locomotor circuits occurs in the absence of supraspinal input in adult rats. Cats with SCI can recover hindlimb locomotion when lumbosacral circuits have access to sensory information^{8,15}. This is usually attributed to the sensory systems providing feedback correction²⁴ and reinforcement²⁵ of motor patterns generated by the spinal circuitry^{4,9,26}. However, the precise contributions of sensory input during spinal locomotion have not been defined. To investigate the influence of sensory input on the initiation and control of standing and stepping in the absence of supraspinal input, we imposed substantial changes in the patterns of afferent information while the rats' spinal circuits were engaged by the full combination of interventions. For this purpose, an additional group of rats ($n = 6$) was trained to step for 3 weeks before testing (Supplementary Fig. 2).

We first compared the effects of dynamic versus static patterns of sensory input. In the absence of treadmill motion, but under weight-bearing conditions ($37\% \pm 3\%$ of weight bearing),

pharmacological and EES interventions facilitated the tonic recruitment of extensor muscles, whereas the flexor muscles were quiescent or weakly active, behaviorally apparent as standing (Fig. 6a). When treadmill belt motion (5 cm s^{-1}) was initiated, all hindlimb joints underwent changes toward extension (limb moving backward), creating dynamic proprioceptive input that immediately transformed the motor patterns from a tonic to a rhythmic state (Fig. 6a). To further test the influence of velocity-dependent afferent input on motor pattern formation, we incrementally increased the treadmill belt speed from 5 cm s^{-1} (slow walking) to 25 cm s^{-1} (running). Increasing treadmill speed induced a velocity-dependent lengthening of the stride ($P < 0.01$; Fig. 6a), an increase in stepping frequency ($P < 0.001$; Fig. 6a,b), a progressive decrease in the duration of the stance phase ($P < 0.001$; Fig. 6b) and of extensor EMG bursts ($P < 0.001$; Fig. 6c), and a progressive adjustment in the relative timing between hindlimb segment oscillations ($P < 0.05$; Fig. 6d). In contrast, the duration of the swing phase (Fig. 6b) and of flexor bursts (Fig. 6c) were unchanged across speeds. Similar adjustments of the kinematics and EMG parameters were observed in noninjured rats (Supplementary Fig. 6). All of the rats with SCI ($n = 6$) accommodated displacement of the limbs and recruitment of motor pools to changing treadmill belt speeds in a single step and were able to locomote for extended periods of time on the treadmill even at the fastest speeds (25 cm s^{-1} ; Supplementary Fig. 7). When the treadmill belt was stopped at either slow or fast speeds, rhythmic hindlimb movements arrested instantly (Fig. 6a). Ongoing bursts in extensor muscles persisted as sustained tonic activity, whereas flexor muscles became quiescent, similar to what would occur in noninjured rats.

Next, we assessed the influence of weight-bearing input on the formation of motor patterns in rats with SCI (Fig. 7). When hindlimbs were suspended above the treadmill belt, that is, in the absence of load-related input, pharmacological and EES interventions induced step-like movements with alternate recruitment of extensor and flexor motor pools in all of the rats ($n = 6$; Fig. 7a). In the absence of belt motion, contact of the hindlimbs with the treadmill immediately arrested the rhythmic movements (Fig. 7a), stopped the recruitment of flexor muscles ($P < 0.001$; Fig. 7d), and induced tonic levels of EMG activity in extensor muscles ($P < 0.001$; Fig. 7d) that resulted in vertical reaction forces ($P < 0.001$; Fig. 7e), enabling a sustained standing posture. Stepping movements continued if the treadmill belt was moving at the time of hindlimb contact, even with minimal weight bearing (Fig. 7b). Increasing the level of weight bearing resulted in a progressive increase in the amplitude of the extensor bursts ($P < 0.001$; Fig. 7b–d), an increase in the vertical reaction forces during stance ($P < 0.001$; Fig. 7b,c,e) and adjustments in hindlimb endpoint trajectories (longer stride, lower height) ($P < 0.01$; Fig. 7b).

Finally, we assessed the effects of direction-dependent afferent input on locomotor pattern formation (Fig. 8). When reversing the direction of the treadmill belt from forward to backward, all of the rats ($n = 6$) showed alternate stepping movements with backward-oriented motion of the foot during swing ($P < 0.001$; Fig. 8b) and significant adaptations (timing and amplitude, $P < 0.001$) in muscle activity (Fig. 8b). Notably, a substantial coactivation of antagonist muscles was observed systematically during stance (Fig. 8b), as also occurred, although less frequently, in noninjured rats (Supplementary Fig. 6). In contrast, reciprocal recruitment of extensor and flexor motor pools was the only pattern observed during forward locomotion (Fig. 8a). Likewise, rotating the rat perpendicular to the treadmill belt direction did not arrest stepping movements. Instead, all of the rats ($n = 6$) showed sideways displacements of the feet ($P < 0.001$; Fig. 8c) with a reversed pattern of hip abduction and adduction ($P < 0.001$; Fig. 8c) compared with forward locomotion (Fig. 8a). Although variable among rats, a major reorganization in the coordination patterns of proximal and distal flexor and extensor motor pools was observed during sideways locomotion. Well-defined coactivation patterns (Fig. 8c) between motor pools that were activated reciprocally during forward locomotion (Fig. 8a) also occurred during sideways stepping. These results reveal a previously unrecognized ability of

velocity-, load- and direction-dependent sensory inputs to regulate both the control of standing and the control of adaptive and flexible stepping movements with an exquisite degree of refinement and without any influences from supraspinal centers in adult rats (Supplementary Video 3).

Discussion

Accessing the circuits and receptors in lumbosacral spinal cord

Although several studies have documented the potential of pharmacological^{9,10} and/or electrical stimulation^{11–14,19,27}, as well as motor training^{2,8,16}, to facilitate stepping in rats with a complete spinal cord transection, limited weight-bearing capacities have been achieved, and when investigated in detail, kinematics and EMG patterns differed substantially from those underlying voluntary stepping. A major result of our study is that a combination of pharmacological and electrical stimulations was able to acutely transform rodent lumbosacral circuits from nonfunctional to highly functional and adaptive states as early as 1 week post-injury. Furthermore, we found that, in conjunction with rehabilitative motor training, the same combined stimulations promoted the recovery of full weight-bearing hindlimb locomotion on a treadmill that was nearly indistinguishable from voluntary stepping, although robotic assistance was necessary for the rats to maintain balance. Together with previous evidence in cats²⁴, our results indicate that the mammalian lumbosacral spinal cord contains circuitry that is sufficient to generate close-to-normal hindlimb locomotor patterns in the absence of any supraspinal input.

The mechanisms underlying locomotion induced by intraspinal stimulation^{13,14} or EES^{11,12,19,27} in rats and cats remain undetermined. Neurophysiological recordings²⁸ and computer simulations²⁹, however, suggest that the electrical stimulation engages spinal circuits primarily by recruiting afferent fibers. In fact, dorsal root stimulation can induce stepping similar to intraspinal stimulation in spinal cord-injured cats¹⁴. In humans, leg muscle vibration, which recruits large-diameter afferent fibers, can evoke locomotor-like movements of the legs⁶. In principle, EES applied at discrete lumbosacral locations could recruit both long-range ascending and descending afferent branches in the segments below the spinal cord transection and activate profuse intraspinal ramifications that contact subsets of circuits localized around the stimulation site³⁰. Accordingly, although electrical stimulation of virtually any lumbosacral segment can facilitate step-like movements on a treadmill¹¹, we found clear site-specific effects of EES on hindlimb locomotion. Consistent with the rostrocaudal anatomical gradient of flexor and extensor motor pools, lumbar stimulation facilitated flexion, whereas stimulation applied at the sacral level primarily facilitated extension. Distinct locations of serotonin receptors associated with stepping have also been reported in neonatal rats. A previous study¹⁸ found that *in vitro* brainstem-induced fictive locomotion can be blocked by antagonizing 5-HT_{2A} or 5-HT₇ receptors and that 5-HT₇ receptors are prominent in the upper lumbar segments, whereas 5-HT_{2A} receptors are more localized to the lower lumbar and sacral segments. Further studies will be required to identify the location and types of neurons, interneurons and receptors that are engaged by serotonergic agonists and electrical stimulation during treadmill locomotion. Nevertheless, our statistical analyses indicate that each pharmacological or electrical intervention modulates distinct functions, suggesting the fine-tuning of selective circuits. This specificity provides the means for the synergy between serotonergic agonist and electrical stimulation interventions, such that only combinations of both were able to functionally engage spinal locomotor networks 1 week after injury and induce substantial functional improvements when combined with rehabilitative locomotor training.

These findings support the viewpoint^{17,31,32} that the spinal motor infrastructure is composed of a widely distributed and heterogeneous, but highly integrated and synergistic, system of neural circuits and receptors that can generate a range of task-specific movements when

recruited in different combinations. Evidence for such principles has been extracted statistically in humans^{33,34} and documented directly in anesthetized frogs³¹, rats³² and cats³⁵. Our findings are consistent with and extend these organizational principles to the production of adaptive locomotor movements without any brain input *in vivo*. Consistent with this, the development of high-density electrode arrays that enable detailed, distributed and simultaneous access to the diffusely located components of the lumbosacral circuits may offer the potential to promote a higher level of motor control than is currently possible in paralyzed subjects.

Functional remodeling of the spinal locomotor circuitry

A substantial reorganization of propriospinal circuits and spared descending fibers that leads to functional recovery occurs spontaneously after an incomplete SCI³ and can be enhanced with locomotor training³⁶. However, there has been limited or no evidence for a similar plasticity of lumbosacral networks when the lesion interrupts all supraspinal inputs in adult rats^{1,2} and humans³⁷, contrary to functional improvements that have been repeatedly documented in cats with SCI^{8,15,16}. We found that the combination of locomotor training with pharmacological and electrical stimulation markedly improved the functional capabilities of the sensorimotor circuits to sustain locomotion without supraspinal input. Although locomotor training with either pharmacological or electrical stimulation alone could reduce the deterioration of stepping ability observed in chronic untrained rats with SCI, only the combination of all three intervention types could produce a substantial improvement. The decrease in the number of FOS-positive neurons, together with elevated synaptic efficacy of monosynaptic inputs to both flexor and extensor motoneuron pools, suggests that locomotor training combined with serotonergic and electrical stimulations may reinforce selected spinal circuits and may suppress other, nonspecific circuitry. Use-dependent selection and strengthening of neural circuits has been shown neurochemically¹⁶ and electrophysiologically^{20,21} after motor training in adult cats with SCI and rats with a neonatal SCI, as well as in the brain in conjunction with the practice of skilled movements³⁸. Our results suggest that similar mechanisms underlie motor learning in the adult rat spinal cord bereft of brain input and that the extent of this functional remodeling is highly correlated with the degree of improvement of locomotor ability. We also found that the chronic absence of activity leads to a deterioration in stepping ability, as has been reported in cats¹⁵. These results corroborate clinical insights from individuals with severe SCI³⁹ and emphasize the need to counteract the rapid deterioration of function that occurs in the absence of weight bearing and motor activity after a SCI.

Combined, these results indicate that the recovery of stepping ability after a spinal cord transection does not result simply from the activation of an ontogenetically defined hardwired and unmodified circuitry that persists and recovers post-injury. Instead, specific combinations of locomotor training and pharmacological and electrical stimulation induce *de novo* use-dependent functional states that enable spinal circuits to learn the motor tasks that are trained and practiced.

Sensory control of stepping after the loss of brain input

The recovery of hindlimb locomotion in animals with SCI is usually attributed to the neuronal networks responsible for central pattern generation, that is, oscillatory output without brain or sensory input^{4,9,26}. However, we found that near normal adaptive stepping and standing without any brain input emerged *in vivo* as a result of the capability of spinal neuronal networks to recognize and use task-specific sensory input. We found that sensory information instantly transformed motor patterns in response to changing task, load, speed and direction conditions with a degree of flexibility and precision that has not been previously observed in animals with SCI²⁴.

Although the role of sensory information in feedback modulation of locomotor activity has been well recognized in cats with SCI^{15,16,24,25} as well as in humans^{40,41}, our results suggest that the sensory information is also instructive in a functional, primary feedforward manner. Indeed, we previously showed that pharmacological and electrical stimulations fail to elicit rhythmic recruitment of deafferented hindlimb muscles in rats with SCI *in vivo*⁴² and a partial deprivation of cutaneous input strongly reduces the stepping ability of cats with SCI, but not in intact cats⁴³. Robust changes in the functional properties of spinal locomotor circuits have been described in the lamprey when introducing sensory inputs⁴⁴. However, these interactions between feedforward and feedback mechanisms have received little attention. Our results indicate that the ability of afferent information to markedly reorganize functional connections among spinal sensorimotor pathways, both acutely and chronically, is an important property of the spinal motor infrastructure.

Clinical perspectives

Our findings have important implications for the understanding of motor pattern formation in the absence of supraspinal input *in vivo* and provide a conceptual framework for the design of strategies to ameliorate motor function in humans after SCI or in the context of other neuromotor disorders such as Parkinson's disease⁴⁵. Preliminary clinical studies have reported that EES can engage lumbosacral circuits of spinal cord-injured individuals⁷ and facilitate the recovery of functional walking⁴⁶. Given the evidence that afferents can serve as a source of control for stepping and standing and can drive use-dependent plasticity of locomotor networks in spinal cord-injured individuals³⁷, combinatorial strategies may also promote recovery of motor function after severe SCI in humans. Such interventions could include neuroprosthetic spinal cord electrode arrays, customized pharmacological treatments and robotically-assisted locomotor training procedures. With the development of efficacious neural repair therapies, these neurorehabilitative strategies may become important for counteracting chronic deterioration of function³⁹, optimizing the use of intrinsic lumbosacral circuits in regaining function³⁷ and ensuring functional interactions between spinal mechanisms and regenerative fibers^{47,48}.

Methods

Methods and any associated references are available in the online version of the paper at <http://www.nature.com/natureneuroscience/>.

Supplementary Material

Refer to Web version on PubMed Central for supplementary material.

Acknowledgments

We would like to acknowledge the excellent technical help provided by S. Zdunowski, L. Friedli, J. Heutschi and O. Märzendorfer for data collection and analysis, as well as M. Herrera for his expert assistance and guidance involving the care and handling of the animals. This work was supported by the Craig H. Nielsen Foundation (#20062668), the International Paraplegic Foundation (P106), the National Center of Competence in Research 'Neural Plasticity and Repair' of the Swiss National Science Foundation, the Christopher and Dana Reeve Foundation (VEC-2007), the US National Institute of Neurological Disorders and Stroke (NS16333), the US Civilian Research and Development Foundation (RUB1-2872-07), the Roman Reed Spinal Cord Injury Research Fund of California and the Russian Foundation for Basic Research (07-04-00526 and 08-04-00688).

References

1. Kubasak MD, et al. OEG implantation and step training enhance hindlimb-stepping ability in adult spinal transected rats. *Brain* 2008;131:264–276. [PubMed: 18056162]

2. Ichiyama RM, et al. Step training reinforces specific spinal locomotor circuitry in adult spinal rats. *J Neurosci* 2008;28:7370–7375. [PubMed: 18632941]
3. Courtine G, et al. Recovery of supraspinal control of stepping via indirect propriospinal relay connections after spinal cord injury. *Nat Med* 2008;14:69–74. [PubMed: 18157143]
4. Grillner S. Biological pattern generation: the cellular and computational logic of networks in motion. *Neuron* 2006;52:751–766. [PubMed: 17145498]
5. Kiehn O. Locomotor circuits in the mammalian spinal cord. *Annu Rev Neurosci* 2006;29:279–306. [PubMed: 16776587]
6. Gurfinkel VS, Levik YS, Kazennikov OV, Selionov VA. Locomotor-like movements evoked by leg muscle vibration in humans. *Eur J Neurosci* 1998;10:1608–1612. [PubMed: 9751133]
7. Dimitrijevic MR, Gerasimenko Y, Pinter M. Evidence for a spinal central pattern generator in humans. *Ann NY Acad Sci* 1998;860:360–376. [PubMed: 9928325]
8. Chau C, Barbeau H, Rossignol S. Early locomotor training with clonidine in spinal cats. *J Neurophysiol* 1998;79:392–409. [PubMed: 9425208]
9. Antri M, Mouffle C, Orsal D, Barthe JY. 5-HT_{1A} receptors are involved in short- and long-term processes responsible for 5-HT-induced locomotor function recovery in chronic spinal rat. *Eur J Neurosci* 2003;18:1963–1972. [PubMed: 14622228]
10. Landry ES, et al. Contribution of spinal 5-HT_{1A} and 5-HT₇ receptors to locomotor-like movement induced by 8-OHDPAT in spinal cord–transected mice. *Eur J Neurosci* 2006;24:535–546. [PubMed: 16836640]
11. Ichiyama RM, Gerasimenko YP, Zhong H, Roy RR, Edgerton VR. Hindlimb stepping movements in complete spinal rats induced by epidural spinal cord stimulation. *Neurosci Lett* 2005;383:339–344. [PubMed: 15878636]
12. Gerasimenko YP, et al. Epidural spinal cord stimulation plus quipazine administration enable stepping in complete spinal adult rats. *J Neurophysiol* 2007;98:2525–2536. [PubMed: 17855582]
13. Guevremont L, et al. Locomotor-related networks in the lumbosacral enlargement of the adult spinal cat: activation through intraspinal microstimulation. *IEEE Trans Neural Syst Rehabil Eng* 2006;14:266–272. [PubMed: 17009485]
14. Barthélemy D, Leblond H, Rossignol S. Characteristics and mechanisms of locomotion induced by intraspinal microstimulation and dorsal root stimulation in spinal cats. *J Neurophysiol* 2007;97:1986–2000. [PubMed: 17215509]
15. De Leon RD, Hodgson JA, Roy RR, Edgerton VR. Retention of hindlimb stepping ability in adult spinal cats after the cessation of step training. *J Neurophysiol* 1999;81:85–94. [PubMed: 9914269]
16. Tillakaratne NJ, et al. Use-dependent modulation of inhibitory capacity in the feline lumbar spinal cord. *J Neurosci* 2002;22:3130–3143. [PubMed: 11943816]
17. Hochman, S.; Garraway, S.; Machacek, D.; Shay, B. 5-HT receptors and the neuromodulatory control of spinal cord function. In: Cope, TC., editor. *Motor Neurobiology of the Spinal Cord*. CRC Press; Boca Raton, Florida: 2001. p. 47-87.
18. Liu J, Jordan LM. Stimulation of the parapyramidal region of the neonatal rat brain stem produces locomotor-like activity involving spinal 5-HT₇ and 5-HT_{2A} receptors. *J Neurophysiol* 2005;94:1392–1404. [PubMed: 15872068]
19. Lavrov I, et al. Epidural stimulation induced modulation of spinal locomotor networks in adult spinal rats. *J Neurosci* 2008;28:6022–6029. [PubMed: 18524907]
20. Petruska JC, et al. Changes in motoneuron properties and synaptic inputs related to step training after spinal cord transection in rats. *J Neurosci* 2007;27:4460–4471. [PubMed: 17442831]
21. Côté MP, Gossard JP. Step training–dependent plasticity in spinal cutaneous pathways. *J Neurosci* 2004;24:11317–11327. [PubMed: 15601938]
22. Barthélemy D, Leblond H, Provencher J, Rossignol S. Nonlocomotor and locomotor hindlimb responses evoked by electrical microstimulation of the lumbar cord in spinalized cats. *J Neurophysiol* 2006;96:3273–3292. [PubMed: 16943319]
23. Lavrov I, et al. Plasticity of spinal cord reflexes after a complete transection in adult rats: relationship to stepping ability. *J Neurophysiol* 2006;96:1699–1710. [PubMed: 16823028]

24. Rossignol S, Dubuc R, Gossard JP. Dynamic sensorimotor interactions in locomotion. *Physiol Rev* 2006;86:89–154. [PubMed: 16371596]
25. Pearson KG. Generating the walking gait: role of sensory feedback. *Prog Brain Res* 2004;143:123–129. [PubMed: 14653157]
26. Barrière G, Leblond H, Provencher J, Rossignol S. Prominent role of the spinal central pattern generator in the recovery of locomotion after partial spinal cord injuries. *J Neurosci* 2008;28:3976–3987. [PubMed: 18400897]
27. Iwahara T, Atsuta Y, Garcia-Rill E, Skinner RD. Spinal cord stimulation-induced locomotion in the adult cat. *Brain Res Bull* 1992;28:99–105. [PubMed: 1540851]
28. Gaunt RA, Prochazka A, Mushahwar VK, Guevremont L, Ellaway PH. Intraspinal microstimulation excites multisegmental sensory afferents at lower stimulus levels than local alpha-motoneuron responses. *J Neurophysiol* 2006;96:2995–3005. [PubMed: 16943320]
29. Rattay F, Minassian K, Dimitrijevic MR. Epidural electrical stimulation of posterior structures of the human lumbosacral cord. 2. Quantitative analysis by computer modeling. *Spinal Cord* 2000;38:473–489. [PubMed: 10962608]
30. Rudomin P. Central control of information transmission through the intraspinal arborizations of sensory fibers examined 100 years after Ramon y Cajal. *Prog Brain Res* 2002;136:409–421. [PubMed: 12143398]
31. Giszter SF, Mussa-Ivaldi FA, Bizzi E. Convergent force fields organized in the frog's spinal cord. *J Neurosci* 1993;13:467–491. [PubMed: 8426224]
32. Tresch MC, Bizzi E. Responses to spinal microstimulation in the chronically spinalized rat and their relationship to spinal systems activated by low-threshold cutaneous stimulation. *Exp Brain Res* 1999;129:401–416. [PubMed: 10591912]
33. Courtine G, Schieppati M. Tuning of a basic coordination pattern constructs straight-ahead and curved walking in humans. *J Neurophysiol* 2004;91:1524–1535. [PubMed: 14668296]
34. Ivanenko YP, Cappellini G, Dominici N, Poppele RE, Lacquaniti F. Modular control of limb movements during human locomotion. *J Neurosci* 2007;27:11149–11161. [PubMed: 17928457]
35. Lemay MA, Grill WM. Modularity of motor output evoked by intraspinal microstimulation in cats. *J Neurophysiol* 2004;91:502–514. [PubMed: 14523079]
36. Engesser-Cesar C, et al. Wheel running following spinal cord injury improves locomotor recovery and stimulates serotonergic fiber growth. *Eur J Neurosci* 2007;25:1931–1939. [PubMed: 17439482]
37. Harkema SJ. Plasticity of interneuronal networks of the functionally isolated human spinal cord. *Brain Res Rev* 2008;57:255–264. [PubMed: 18042493]
38. Rioult-Pedotti MS, Friedman D, Donoghue JP. Learning-induced LTP in neocortex. *Science* 2000;290:533–536. [PubMed: 11039938]
39. Dietz V, Muller R. Degradation of neuronal function following a spinal cord injury: mechanisms and countermeasures. *Brain* 2004;127:2221–2231. [PubMed: 15269117]
40. Harkema SJ, et al. Human lumbosacral spinal cord interprets loading during stepping. *J Neurophysiol* 1997;77:797–811. [PubMed: 9065851]
41. Beres-Jones JA, Harkema SJ. The human spinal cord interprets velocity-dependent afferent input during stepping. *Brain* 2004;127:2232–2246. [PubMed: 15289272]
42. Lavrov I, et al. Facilitation of stepping with epidural stimulation in spinal rats: role of sensory input. *J Neurosci* 2008;28:7774–7780. [PubMed: 18667609]
43. Bouyer LJ, Rossignol S. Contribution of cutaneous inputs from the hindpaw to the control of locomotion. II. Spinal cats. *J Neurophysiol* 2003;90:3640–3653. [PubMed: 12944535]
44. Grillner S, Wallen P. Cellular bases of a vertebrate locomotor system—steering, intersegmental and segmental coordination and sensory control. *Brain Res Brain Res Rev* 2002;40:92–106. [PubMed: 12589909]
45. Fuentes R, Petersson P, Siesser WB, Caron MG, Nicolelis MA. Spinal cord stimulation restores locomotion in animal models of Parkinson's disease. *Science* 2009;323:1578–1582. [PubMed: 19299613]

46. Carhart MR, He J, Herman R, D'Luzansky S, Willis WT. Epidural spinal-cord stimulation facilitates recovery of functional walking following incomplete spinal-cord injury. *IEEE Trans Neural Syst Rehabil Eng* 2004;12:32–42. [PubMed: 15068185]
47. Courtine G, et al. Can experiments in nonhuman primates expedite the translation of treatments for spinal cord injury in humans? *Nat Med* 2007;13:561–566. [PubMed: 17479102]
48. Maier IC, et al. Differential effects of anti-Nogo-A antibody treatment and treadmill training in rats with incomplete spinal cord injury. *Brain* 2009;132:1426–1440. [PubMed: 19372269]

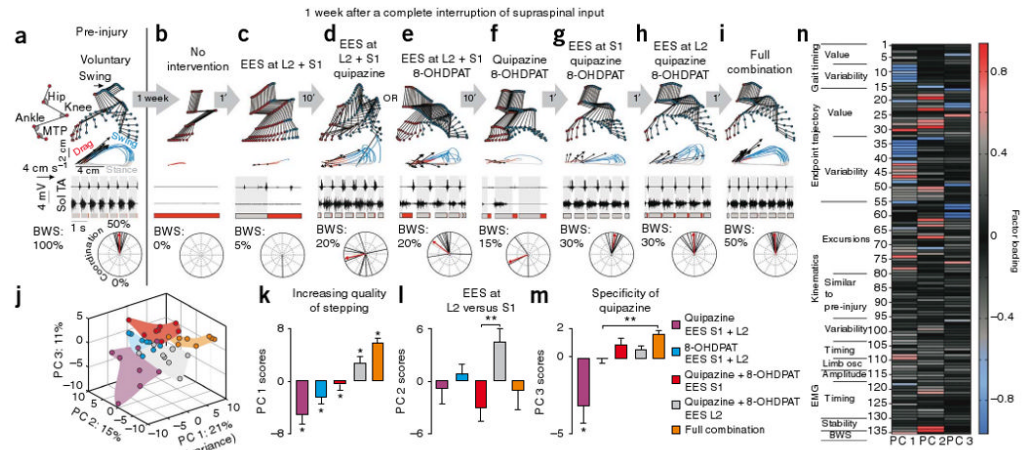


Figure 1.

Accessing spinal locomotor circuits 1 week after the interruption of all supraspinal input. (a–i) EMG and kinematic characteristics underlying locomotion recorded pre-injury (a) and 7–8 d post-injury (b) without any intervention, as well as under various combinations of serotonergic agonists and/or EES (c–i). The full combination (i) included quipazine, 8-OHDPAT and EES at L2 and S1. Recordings were performed sequentially in the same rat. Horizontal arrows indicate the chronology of the different recordings. A representative stick diagram decomposition of hindlimb motion during swing is shown for each condition with successive color-coded trajectories of limb endpoint. Vectors represent the direction and intensity of the limb endpoint velocity at swing onset. A sequence of raw EMG activity from tibialis anterior (TA) and soleus (Sol) muscles is shown below. Grey and red bars indicate the duration of stance and drag phases, respectively. The BWS of the represented rat under each condition is shown. Finally, a polar plot representation documents the coordination between the left and right hindlimbs (thin arrow, single gait cycle; thick red arrow, average of all gait cycles; 50%, out of phase). (j) Three-dimensional statistical representation of locomotor patterns. Each small colored label represents the gait pattern from an individual rat under a given combination of interventions. The area defined by individual points under a given condition is traced to emphasize the differences between gait patterns under specific combinations. This analysis revealed that each combination of interventions resulted in distinct, but reproducible, patterns of locomotion. (k–m) Bar graphs of average scores on principal components 1–3. (n) Color-coded representation of factor loadings that identify the variables that contributed most to the differences observed between the experimental conditions. For example, principal component 2 captured the differences between stepping with EES at L2 versus S1. Variables associated with changes in joint angles toward flexion and limb endpoint trajectory (left and right step heights, 18–19) clustered on principal component 2, indicating that EES at L2 enhanced flexion, whereas EES at S1 enhanced extension. All of the computed kinematic and EMG variables ($n = 135$) are reported in Supplementary Table 1. Error bars represent s.e.m. * $P < 0.05$, different from all other conditions. ** $P < 0.05$, significantly different conditions.

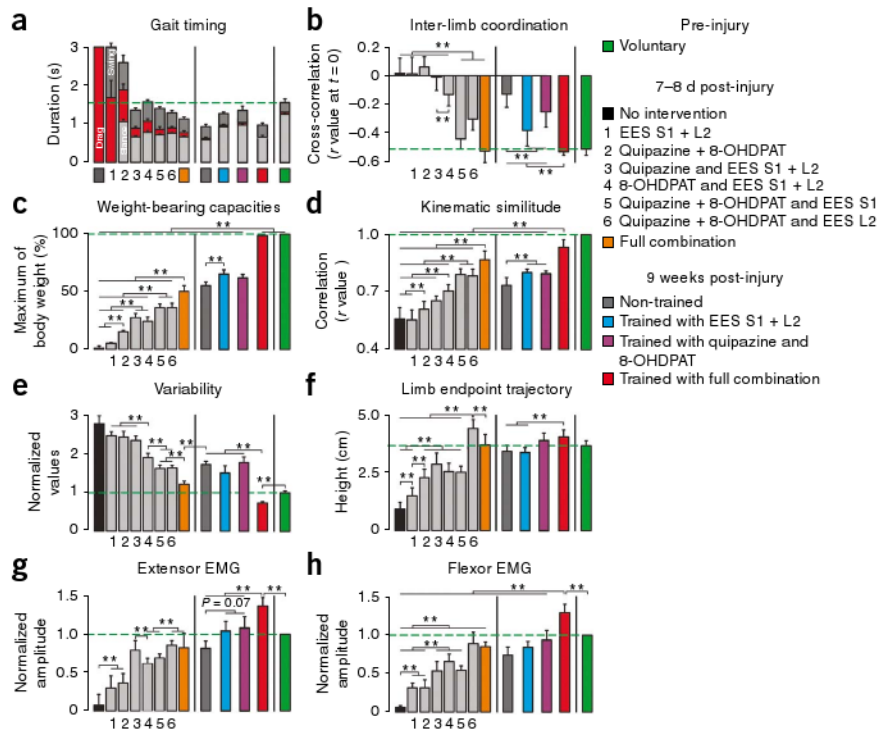


Figure 2. Kinematics and EMG features of locomotor patterns. **(a–h)** Bar graphs of average values ($n = 7$ or 8 rats per group) for locomotor parameters computed under the different experimental conditions. In each graph, the green horizontal bar represents the pre-lesion baseline recorded in the same rat 1 week pre-injury. The duration of stance (light gray), swing (dark gray) and drag (red) phases is shown in **a**. The r values at $t = 0$ for the cross-correlation function between oscillations of the left and right hindlimbs computed over a gait sequence of ten steps is shown in **b**. A r value of -0.5 indicates out of phase coupling between the limbs. The maximum level of weight bearing (percentage of body weight) at which the rat could perform ten successful steps is shown in **c**. Cross-correlation functions were computed between datasets obtained pre-injury and under a given experimental condition for the hip, knee, ankle and MTP joint angles, and associated joint velocity profiles (**d**). Maximum r values were extracted from each cross-correlation function and averaged across joint angle and joint angle velocity profiles. The variability of gait parameters computed as the mean coefficient of variation for all the computed parameters normalized to the pre-injury baseline are shown in **e**. Step height, defined as the maximum vertical distance between the foot (MTP marker) and the stepping surface, is shown in **f**. The average EMG burst amplitude for left and right soleus (**g**) and tibialis (**h**) anterior muscles normalized to pre-injury values are shown. Error bars represent s.e.m. ** $P < 0.05$, significantly different conditions.

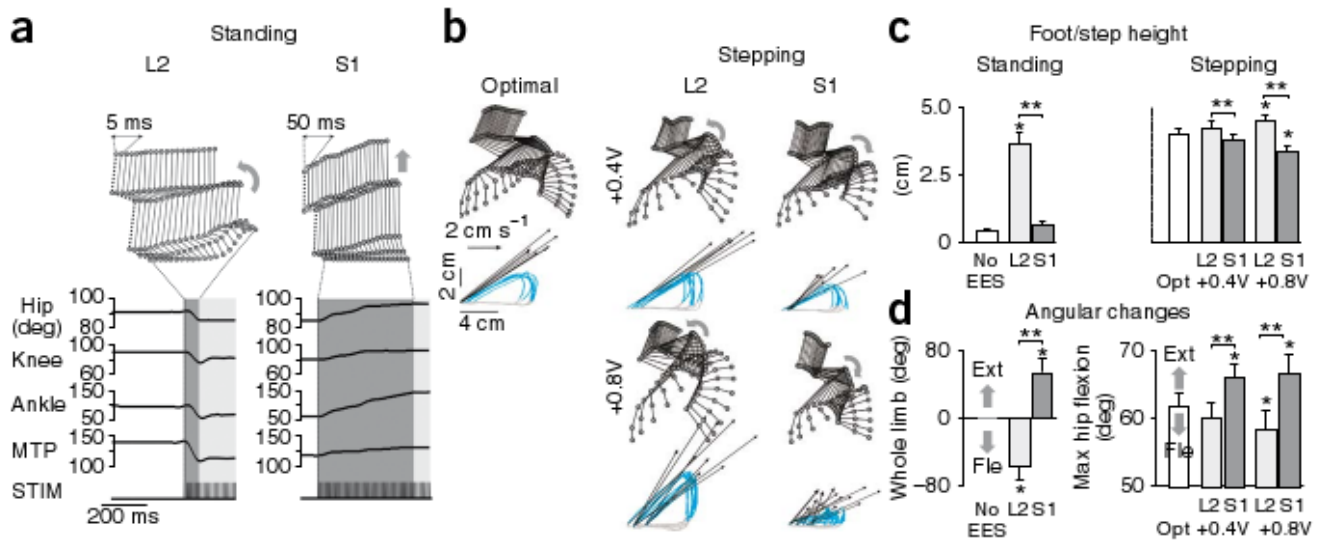


Figure 3.

Site-specific effects of EES during standing and stepping. **(a)** Stick diagram decomposition of hindlimb movements and time course of changes in hindlimb joint angles when delivering EES at L2 (left) or S1 (right) during standing (20% of weight bearing). Each diagram is separated by 5 ms (L2) or 50 ms (S1). The dark gray shaded areas indicate the period during which EES-induced changes in hindlimb posture were observed. Light gray shaded areas represent periods during which EES-induced posture was maintained. **(b)** Effects of increasing EES by 0.4 and 0.8 V at L2 versus S1 on hindlimb movements during locomotion enabled by the full combination of interventions. Data are presented as in Figure 1. Arrows indicate increased flexion with EES at L2 versus increased extension with EES at S1. **(c)** Bar graph of average values of maximum foot height during standing and step height during locomotion. Opt, optimal EES intensity to encourage stepping. **(d)** Bar graphs of average values of angular changes during standing and stepping. For standing, values were obtained by measuring, for each joint angle, the difference between positions at EES onset and at the time of maximum EES-induced change in hindlimb posture at each joint and then averaging these values across joints. Ext, extension. Fle, flexion. For stepping, the maximum position of the hip joint angle in flexion during swing was computed. Error bars represent s.e.m. * $P < 0.05$, different from all the other conditions. ** $P < 0.05$, significantly different conditions.

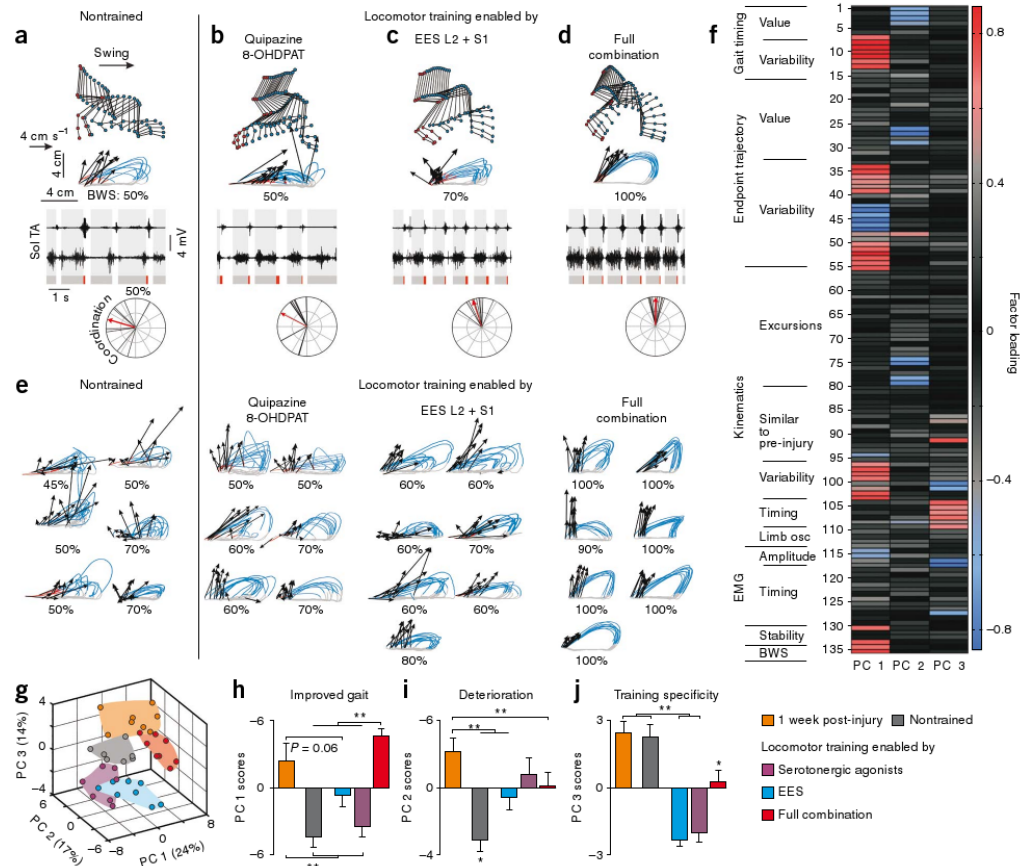
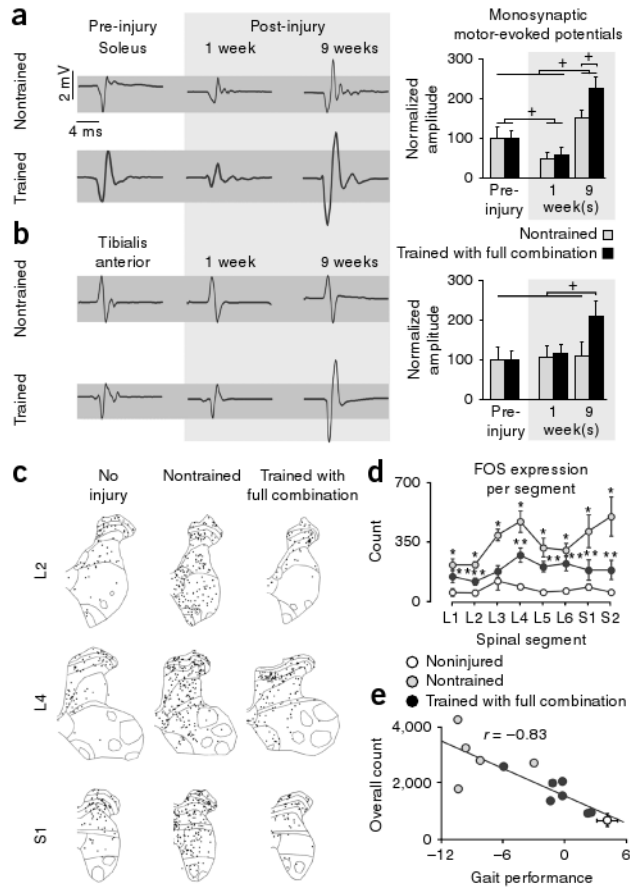


Figure 4. Rehabilitation locomotor training enabled by pharmacological and EES interventions improves stepping ability. **(a–d)** Representative illustrations of EMG and kinematic characteristics underlying bipedal hindlimb locomotion recorded at 9 weeks post-injury under the full combination of interventions for a nontrained rat with SCI that did not receive pharmacological or EES interventions for the entire duration of the post-injury period until the day of testing **(a)**, a rat with SCI that was trained with serotonergic agonists only **(b)**, a rat with SCI that was trained with EES at L2 and S1 only **(c)**, and a rat with SCI that was trained with the full combination of interventions **(d)**. Data for this rat are also shown pre-injury in Figure 1a and at 1 week post-injury in Figure 1i. **(e)** Successive limb endpoint trajectories from the right hindlimb are shown for all of the other rats from each experimental group. The BWS of each rat is reported below each limb endpoint trajectory. **(f)** Color-coded representation of factor loadings of each variable on principal components 1–3 (as shown in Fig. 1n). Principal component 1 identified improved gait in rats tested at 1 week post-injury and then trained with the full combination compared with the other groups. The analysis of variables that clustered on principal component 1 indicated that reduced variability of gait parameters, improved gait stability, increased amplitude of EMG activity and recovery of full weight-bearing capacities were the more salient features for explaining the improved stepping performances of rats trained with the full combination. **(g)** Three-dimensional statistical representation of locomotor patterns. The near absence of spatial interceptions between the different groups indicates that each group of rats had unique stepping patterns. **(h–j)** Bar graphs of average scores on principal components 1–3, which each captured specific effects. Error bars represent s.e.m. * $P < 0.05$, different from all the other conditions. ** $P < 0.05$, significantly different conditions. Data are presented as in Figure 1.

**Figure 5.**

Functional remodeling of spinal circuits after rehabilitative locomotor training. **(a)** Representative average ($n = 10$) traces of monosynaptic motor-evoked potentials recorded from the soleus muscle pre-injury and at 1 and 9 weeks post-injury. Data are shown for one nontrained and one rat trained with the full combination of interventions. Dark shaded areas indicate the amplitude of pre-injury motor-evoked potentials. Bar graphs report the average amplitude of motor-evoked potentials recorded in the soleus muscle at the different time points. **(b)** Data are presented as in **a** for the tibialis anterior muscle. **(c)** Representative example of camera lucida drawings of FOS-positive cells in spinal segments L2, L4 and S1 of a noninjured rat, a nontrained rat with SCI and a rat with SCI trained with the full combination of interventions. **(d)** Average values for the total FOS-positive cell count (all laminae) per spinal segment. **(e)** Correlation between the total number of FOS-positive cells (all laminae from L1 to S2) and gait performance measured as individual scores along the principal component 1 axis. PCA was applied on locomotor data ($n = 135$) recorded from the same rats 3–5 d before the FOS experiments under the same conditions, that is, no intervention for noninjured rats and under the full combination for rats with SCI. Error bars represent s.e.m. * $P < 0.05$, different from noninjured group. ** $P < 0.05$, different from trained group.

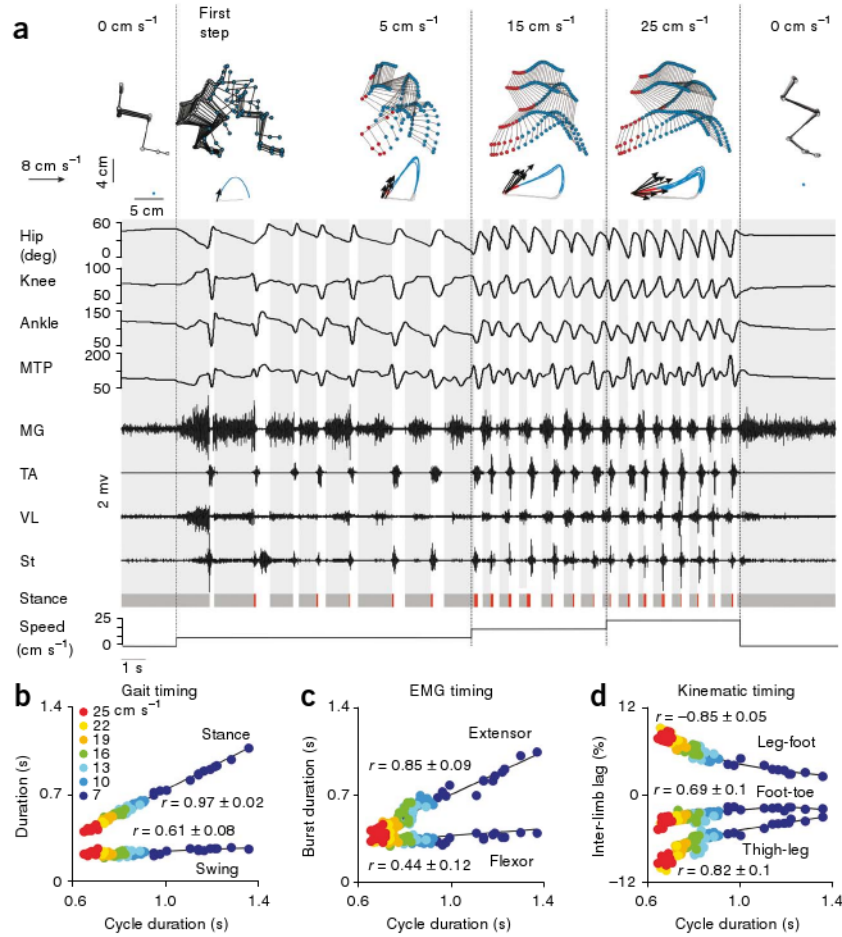
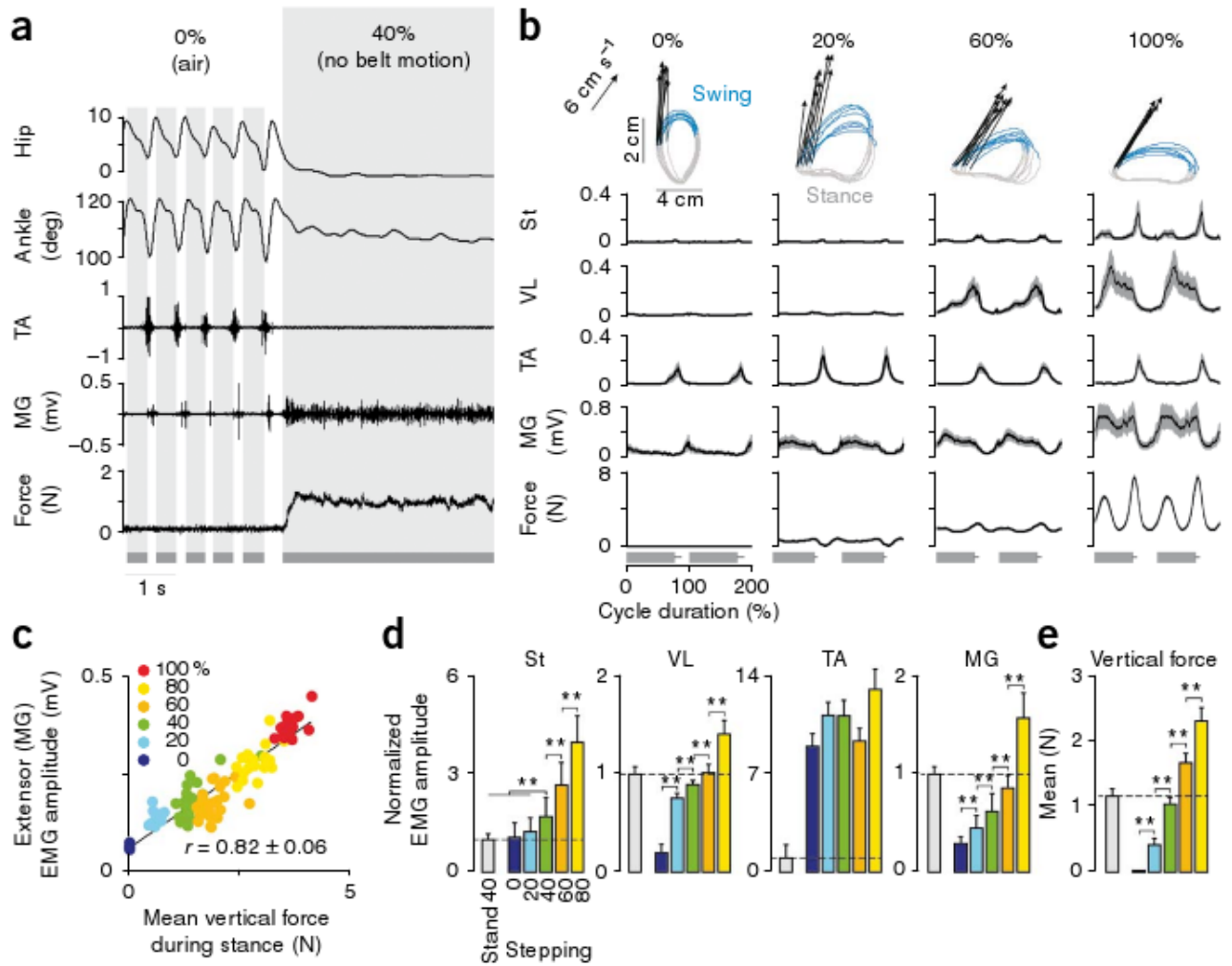


Figure 6. Effects of velocity-dependent afferent input on motor patterns. (a) Representative example of hindlimb kinematics and EMG activity recorded from a continuous sequence of steps during which the speed of the treadmill belt was changed gradually (0, 5, 15, 25 and 0 cm s⁻¹). Data are presented as in Figure 1, except that changes in hindlimb joint angles are also shown. Stick diagram decomposition of the first step is shown to demonstrate the smooth transition from standing to stepping. MG, medial gastrocnemius; St, semitendinosus; VL, vastus lateralis. (b) The durations of the swing and stance phases are plotted against the cycle duration. Color-coded labels indicate the measured treadmill belt speed during the performance of the represented gait cycles. (c) The durations of flexor (TA) and extensor (MG) EMG bursts are plotted against the cycle duration. (d) The temporal lag between oscillations (with respect to the direction of gravity) of adjacent hindlimb segments is plotted against the cycle duration. Inter-limb lags were computed by means of cross-correlation functions and expressed as a percent of cycle duration. **b–d** are shown for a representative rat. Mean \pm s.e.m. correlation values computed by averaging values obtained from linear regressions performed on each rat ($n = 6$) individually are reported in each plot. All rats were trained with the full combination of interventions for 3 weeks before the experimental testing.

**Figure 7.**

Effects of load-dependent afferent input on motor patterns. **(a)** Representative example of hindlimb kinematics and EMG activity induced by the full combination while the rat transitioned from suspended in the air (0% of body weight) to contact with the immobile treadmill belt (40% of body weight support). **(b)** Representative example of limb endpoint trajectories, mean EMG activity and mean vertical reaction forces during stepping with 0, 20, 60 or 100% weight bearing. **(c)** The mean vertical reaction force measured during stance is plotted against the amplitude of the medial gastrocnemius EMG burst for a representative rat that demonstrated full weight-bearing capacities after 3 weeks of training with the full combination of interventions. Color-coded labels represent the amount of body weight supported by the hindlimbs of the rat. A strong relationship was observed in all of the rats ($n = 6$). The mean \pm s.e.m. correlation value computed by averaging the values obtained from linear correlation computed on each rat is reported. **(d)** Bar graphs of average amplitudes ($n = 6$) of EMG bursts in selected hindlimb muscles. Values are normalized to values measured during standing (40% of body weight support). The 100% weight-bearing condition is not represented because only two rats could step without any support after 3 weeks of training. **(e)** Bar graphs of average values ($n = 6$) of vertical reaction forces measured during stance. Error bars represent s.e.m. ****** $P < 0.05$, significantly different conditions.

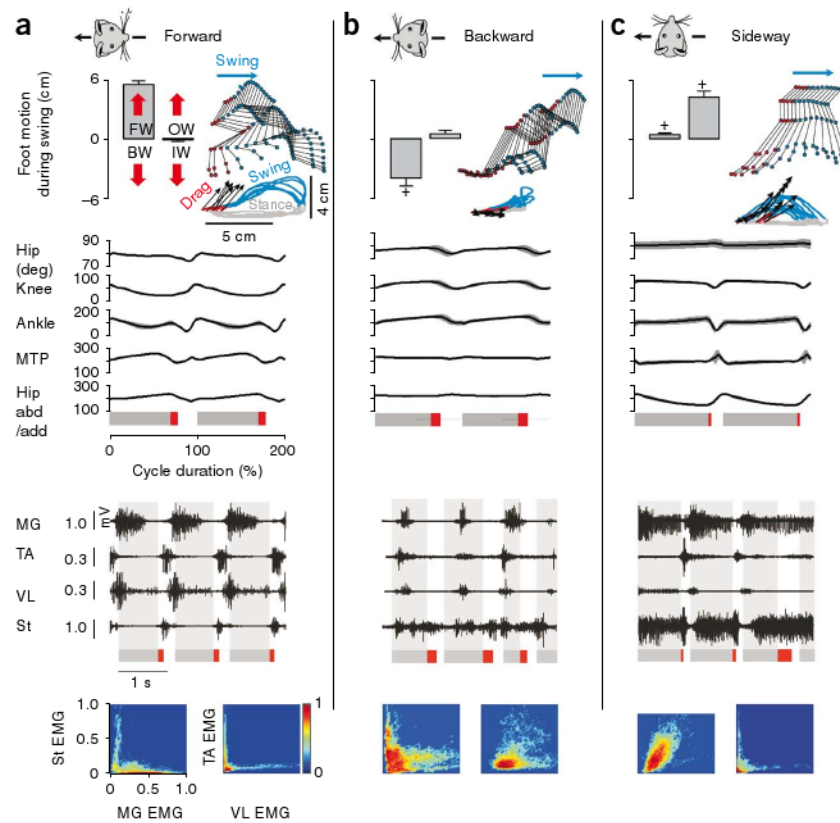


Figure 8.

Effects of direction-dependent afferent input on motor patterns. (a–c) Representative example of mean (+ s.d.) hindlimb kinematics and raw EMG activity during continuous locomotion in the forward (a), backward (b) and sideways (c) directions. The same limb from the same rat is shown for the three directions, which corresponds to the leading (front) limb during sideward locomotion. Bar graphs show the average ($n = 6$ rats) linear distance traveled by the foot during swing with respect to the pelvis orientation for the different directions of stepping. Backward (BW) and forward (FW) motions correspond to displacements in the sagittal plane (defined by the pelvis orientation), whereas outward (OW) and inward (IW) motions correspond to displacements in the medio-lateral direction. Probability density distributions of normalized EMG amplitudes between the semitendinosus and medial gastrocnemius muscles, and the tibialis anterior and vastus lateralis muscles are shown at the bottom. L-shape patterns indicate reciprocal activation between the pair of muscles, whereas line-shape patterns indicate coactivation. Abd, abduction (increasing value); Add, adduction. Data are presented as in Figure 1, except that stick diagrams are represented in three dimensions, with the main plane oriented with the direction of the treadmill belt motion.